BMC Genomics

RESEARCH Open Access

# Integrated multi-omics profiling unveils a network of key signaling pathways governing ovarian function and systemic regulation in high-prolificacy goats

Fan Jiang[1†], Hu Tao[1†], Mengjie Chen[1†], Aishao Shangguan[1†], Haimiao Lv[1], Zaidong Hua[1], Nian Zhang[1], Feng Zhang[1], Tian Xu[1], Wen Wang[1,2], Chengtao Ma[1,3] and Qi Xiong[1*]

## Abstract

**Background** Prolificacy is a crucial economic trait in goat production, yet its underlying molecular mechanisms remain incompletely understood due to its polygenic nature. While previous studies have identified several candidate genes, a comprehensive understanding of the local and systemic regulatory networks is lacking. This study aims to dissect the complex molecular basis of high prolificacy in goats through an integrated multi-omics approach.

**Results** We conducted transcriptomic, proteomic, and metabolomic profiling of ovarian tissues from high-fecundity (HF, $n=3$) and low-fecundity (LF, $n=3$) Chubao black-head goats, alongside multi-tissue (heart, liver, spleen, lung and kidney) transcriptome sequencing. Our analysis identified 1,075 differentially expressed genes (DEGs), 286 differentially expressed proteins (DEPs), and 55 differentially expressed metabolites (DEMs) in the ovary. Functional enrichment highlighted critical roles for signaling pathways such as Hippo, Wnt, MAPK, ECM-receptor interaction, and PI3K-Akt. Integrated cross-omics analysis revealed 10 genes (including *CA3*, *CENPV*, and *GATM*) consistently differentially expressed at both transcriptional and protein levels, and public single-cell RNA (scRNA) sequencing analysis further demonstrated their specific expression in key ovarian cell types including germ cells, granulosa cells, and theca cells. A core regulatory network centered on glycerophospholipid metabolism was constructed, showing coordinated dysregulation of metabolites like PC(20:3(5Z,8Z,11Z)/20:3(8Z,11Z,14Z)) and 1-Palmitoyl-sn-glycero-3-phosphocholine with genes *PLA2G2C* and *PTDSS1*. Multi-tissue transcriptomics further indicated that prolificacy involves both ovary-specific regulation and conserved systemic mechanisms.

**Conclusions** This study demonstrates that high prolificacy in goats is a complex trait co-regulated by key local pathways in the ovary and systemic transcriptional adaptations. Our integrated multi-omics strategy provides

†Fan Jiang, Hu Tao, Mengjie Chen and Aishao Shangguan contributed equally to this work and should be considered co-first authors.

*Correspondence:
Qi Xiong
phenixxq@163.com

Full list of author information is available at the end of the article

a systematic molecular portrait of fecundity, identifying novel candidate genes and biomarkers with potential applications in genetic improvement programs for goats.

**Keywords** Goat, Prolificacy, Ovary, Multi-omics, Glycerophospholipid metabolism

## Background

Reproductive efficiency, particularly prolificacy, represents a fundamental economic trait in goat production systems worldwide, with significant implications for meat, milk, and cashmere yield [1–3]. The physiological basis of prolificacy, defined as the number of offspring per birth, is intrinsically linked to ovarian function, specifically the processes of folliculogenesis, ovulation, and corpus luteum formation. Despite its importance, the molecular mechanisms governing the pronounced differences in litter size between high-fecundity (HF) and low-fecundity (LF) goat breeds remain incompletely elucidated. Traditional candidate gene approaches have identified several mutations associated with increased ovulation rates, such as those in the *BMPR-IB*, *GDF9*, and *BMP15* genes [4–6]. However, these findings explain only a fraction of the observed phenotypic variance, suggesting that prolificacy is a complex polygenic trait regulated by a sophisticated network of genetic, proteomic, and metabolic factors.

Recent advances in high-throughput technologies have enabled systematic investigations of biological systems at multiple levels [7, 8]. To effectively dissect this complexity, studies require a suitable animal model with inherent prolificacy and documented genetic diversity. The Chubao black-head goat, a breed developed by crossing high-meat-yield Boer goats with highly prolific Macheng black goats, provides such a model [9]. It possesses a genetic architecture conducive to high reproduction, and population-level genomic analyses have confirmed substantial genetic variation in its reproductive traits, making it an ideal system for investigating the molecular basis of prolificacy.

Transcriptome sequencing (RNA-Seq) has been extensively employed to profile gene expression landscapes in reproductive tissues. For instance, bulk RNA-seq studies in goats have identified key differentially expressed genes (DEGs) such as *LYPD6, VEGFA*, and *NOS3* in ovaries of high- versus low-fecundity breeds during estrus, elucidating roles in prolactin and Jak-STAT signaling pathways [10]. Similarly, in sheep, comparative transcriptomic analyses between prolific and non-prolific breeds revealed DEGs like *GDF9* and *BMP15* associated with ovulation rate and litter size [11]. Complementarily, single-cell transcriptomic analyses of goat and sheep ovaries have successfully delineated cell-type-specific expression patterns, revealing that genes like *FST*, *CYP19A1*, and *NR5A2* are predominantly expressed in granulosa cells, while *COL1A2* and *LUM* are specific to stromal and theca cells, highlighting their crucial roles in follicular development [12, 13]. In sheep, single-cell RNA (scRNA) sequencing of oocytes from antral follicles uncovered developmentally dynamic networks and key genes such as *ZP3* and *GDF9* governing folliculogenesis [14]. Furthermore, comparative transcriptomic studies between prolific and non-prolific breeds have begun to uncover key DEGs and pathways, yet these studies have often been limited to a single tissue type, overlooking the potential systemic regulatory mechanisms that coordinate reproductive output across the entire organism [15].

To achieve a more holistic understanding, a multi-omics integrative approach is imperative. While transcriptomics provides a blueprint of potential cellular activity, the functional executers are proteins, and the ultimate biochemical phenotypes are reflected in the metabolome. Proteomic studies, such as those utilizing 4D-DIA (Data-Independent Acquisition) mass spectrometry, have revealed significant differences in ovarian protein profiles between breeding and non-breeding seasons in dairy goats, implicating processes like steroid hormone biosynthesis and metabolic pathways in reproductive cyclicity [16]. Similarly, metabolomic profiling via Liquid Chromatography-Mass Spectrometry (LC–MS)/MS has demonstrated its power to identify key metabolic signatures, as evidenced by studies comparing colostrum from high- and low-yielding dairy goats [17]. Nevertheless, a concerted effort integrating transcriptome, proteome, and metabolome data from both ovarian and key peripheral tissues specifically in the context of inherent prolificacy is strikingly absent from the current literature.

Therefore, the primary objective of this study was to conduct a comprehensive multi-omics investigation to unravel the molecular determinants of prolificacy in goats. We performed: 1) RNA-Seq on ovarian tissues from HF and LF goats to identify DEGs; 2) Multi-tissue transcriptome sequencing (heart, liver, spleen, lung and kidney) to elucidate systemic transcriptional regulation; 3) Ovarian proteomic profiling using advanced mass spectrometry to quantify protein abundance differences; and 4) Ovarian metabolomic analysis to characterize the biochemical phenotype. Although the sample size used in this study is limited, it is consistent with the scale of previous multi-omics studies in livestock [12, 13, 18]. This experimental design, combined with the application of stringent statistical thresholds, is considered sufficient for detecting molecular differences with substantial biological effects. By integrating these datasets, we aimed to construct a regulatory network encompassing genes,

proteins, and metabolites, thereby providing unprecedented insights into the complex mechanisms underlying goat prolificacy and identifying robust biomarkers for genetic selection programs.

## Materials and method

### Animals and samples preparation

Six female Chubao black-head goats were selected from the lower goat farm of Hubei Academy of Agricultural Sciences. The animals were divided into two groups: a single-lamb group (LF, $n = 3$), defined as goats that had produced one lamb per parity for at least two consecutive years, and a multiple-lamb group (HF, $n = 3$), defined as those producing two or more lambs per parity over the same period (detailed lambing history is provided in Table S1). All goats underwent synchronized estrus treatment, which included an injection of Pregnant Mare Serum Gonadotropin (PMSG). Ovaries were collected 48 h after PMSG injection, a time point corresponding to the late follicular phase to ensure the capture of molecular signatures associated with synchronized follicular development and impending ovulation. At the end of the experimental period, goats were humanely euthanized via intravenous injection of sodium pentobarbital to ensure deep anesthesia and death without pain. This method was chosen to comply with animal welfare standards and to allow for the immediate collection of intact ovarian tissues for subsequent analysis**.** Following euthanasia, ovary was collected from each animal and stored at −80 °C until further analysis.

### RNA sequencing

Total RNA was extracted from ovarian tissue using TRIzol reagent (Invitrogen). RNA quality was assessed using a NanoDrop spectrophotometer and an Agilent 2100 Bioanalyzer, with all samples exhibiting an RNA Integrity Number (RIN) > 7.0. Sequencing libraries were subsequently constructed using the NEBNext Ultra II Directional RNA Library Prep Kit for Illumina and subjected to paired-end sequencing (150 bp) on an Illumina NovaSeq X Plus platform. All RNA-seq reads obtained were then processed with trimmomatic (version 0.39) [19] to remove adapter and low-quality sequences, and then aligned to *Capra hircus* reference genome (ARS1.2, GCF_001704415.2) using Hisat2 (version 2.2.1) [20]. Read counts per gene were generated with HTSeq (version 2.0.5) [21] based on the corresponding annotation file. The mapped reads count was used to test differential expression with DESeq2 (version 4.3.3) [22]. Genes with a $p$ value < 0.05 and $|\log_2 \text{ratio}| \geq 1$ were considered to be differentially expressed. Gene Ontology (GO) and Kyoto Encyclopedia of Genes and Genomes (KEGG) [23] enrichment analysis of DEGs was performed using KOBAS [24] analysis platform(http://bioinfo.org/kobas/).

### Protein extraction and proteome analysis

Ovarian tissues (HF = 3, LF = 3) were ground in liquid nitrogen and lysed using an SDT buffer containing DTT [25]. After ultrasonication and centrifugation, the supernatant was collected, heat-denatured, and alkylated with iodoacetamide (IAM) in the dark. Proteins were then acetone-precipitated, washed, and redissolved in a dissolution buffer. Protein concentration was determined using a Bradford assay. A standard curve was generated using BSA standards, and sample concentrations were calculated based on absorbance at 595 nm. 20 μg of each protein sample was separated on a 12% SDS-PAGE gel (120 V for 20 min on stacking gel, 150 V for 50 min on separating gel). The gel was stained with Coomassie Brilliant Blue R-250 to visualize protein bands.

The sample was dissolved in mobile phase A (water with 0.1% formic acid), centrifuged, and 200 ng of supernatant was injected into a UHPLC system coupled to a Thermo Orbitrap Astral mass spectrometer. Chromatographic separation was performed using a C18 column with a gradient elution. Mass spectrometry was conducted in data-independent acquisition (DIA) mode with specific settings including a full MS scan range of m/z 380–980 and DIA fragmentation with 300 windows. Raw data were processed using DIA-NN software [26] for protein identification and quantification. Protein quantification results were statistically analyzed using the T-test, and differentially expressed proteins were identified based on statistical significance ($p < 0.05$) and fold change (FC > 1.5 or FC < 0.67) between HF and LF groups. The interaction analysis of the identified proteins was conducted using the StringDB protein interaction database (http://string-db.org/) [27].

### Untargeted metabolomics profiling

Flash-frozen ovarian tissues (100 mg) were homogenized and extracted with prechilled 80% methanol. After vortexing and incubation on ice, samples (3 HF, 3 LF) were centrifuged (15,000 g, 20 min, 4 °C). The supernatant was diluted to 53% methanol with LC–MS grade water, recentrifuged, and the final supernatant was injected for LC–MS/MS analysis [28]. Metabolite separation was performed on a Vanquish UHPLC system coupled to a Q Exactive™ HF/HF-X mass spectrometer, using a Hypersil Gold column (100 × 2.1 mm, 1.9 μm) with a 12 min methanol/water gradient containing 0.1% formic acid. MS data were acquired in both positive and negative ionization modes.

Raw data were processed with XCMS for peak alignment and quantification. Metabolites were identified by accurate mass (≤ 10 ppm) and UHPLC-MS/MS matching against standard databases. After background subtraction and CV-based filtering (QC CV > 30% removed), normalized relative peak areas were obtained. Both positive

and negative ionization modes were employed during LC–MS analysis to ensure robust metabolome profiling and accurate quantification. These metabolites were annotated using the KEGG, HMDB (https://hmdb.ca/metabolites) [29] and LIPIDMaps (http://www.lipidmaps.org/) [30] databases. PLS-DA were performed at metaX [31]. We applied univariate analysis (t-test) to calculate the statistical significance (*p*-value).The metabolites with VIP > 1 and *p*-value < 0.05 and fold change ≥ 1.2 or FC ≤ 0.83 were considered to be differential metabolites. Volcano plots were generated using ggplot2 in R based on $\log_2$(FC) and -$\log_{10}$(*p*-value). Functional and pathway analyses were conducted using the KEGG database.

#### Multi-omics joint analysis

In order to investigate the biological links between the transcriptome/proteome and metabolome, we entered the DEGs, differentially expressed proteins (DEPs), and differentially expressed metabolites (DEMs) into the "Joint Pathway Analysis" module of the MetaboAnalyst [32] database. We conduct two types of analyses on metabolites: one is based on metabolic pathways (only for metabolites), and the other is an analysis covering all pathways (only for genes). Using the Spearman correlation coefficient to quantify differentially expressed genes and proteins, we systematically analyzed the association between the transcriptome and the proteome.

#### RT-qPCR

Total RNA (1 μg) was reverse transcribed into cDNA (20 μL) with a PrimeScript RT Reagent Kit (Takara). The resultant cDNA was subjected to RT-qPCR analysis using TB Green® Premix Ex Taq™ II (Takara), following the manufacturer s' instruction. Relative mRNA level of transcripts was normalized with the *β-actin* mRNA level as reference. Data were presented as mean ± standard deviation of three independent experiments.

## Results

#### Identification of DEGs

We conducted HF and LF ovarian transcriptome profiling using RNA-seq. The cDNA libraries were sequenced using an Illumina platform, producing 484,636,732 raw reads. After quality control filtering, 3.34% of the reads were removed, leaving 468,118,814 clean reads (Table S2). The reads were subsequently mapped to the *Capra hircus* reference genome, with 92.9% to 94.7% of the reads being successfully mapped. A total of 1075 DEGs between HF and LF were identified in this study using a $|\log_2 FC| >= 1$ and p-value < 0.05, of which 533 were up-regulated and 542 down-regulated (Fig. 1A and Table S3). The GO enrichment analysis was conducted on these DEGs, revealing that the up-regulated genes were enriched in pathways such as protein binding, cytoplasm, plasma membrane, cytosol and extracellular region (Fig. 1B and Table S4), while the down-regulated genes were enriched in pathways such as plasma membrane, extracellular space, collagen-containing extracellular matrix and integral component of membrane (Fig. 1C and Table S5). At the same time, KEGG analysis was also conducted, revealing that the up-regulated genes were enriched in the pathways of Glycerophospholipid metabolism, Cytokine-cytokine receptor interaction, Hippo signaling pathway, Wnt signaling pathway, and MAPK signaling pathway (Fig. 1D and Table S6), while the down-regulated genes were enriched in the signaling pathways of ECM-receptor interaction, PI3K-Akt signaling pathway, Neuroactive ligand-receptor interaction, PPAR signaling pathway, Steroid biosynthesis, and HIF-1 signaling pathway (Fig. 1E and Table S7).

#### Multi-tissue analysis identifies DEGs

To elucidate the transcriptional regulatory features underlying prolificacy in goats at a multi-tissue level, we conducted transcriptome sequencing of heart, liver, spleen, lung, kidney, and other tissues from LF and HF goats (Fig. 2A). Using consistent screening criteria ($|\log_2 FC| \geq 1$ and p-value < 0.05) to identify DEGs, we found that the ovary contained the highest number of tissue-specific DEGs, totaling 954, whereas the lung showed the fewest, with only 57 (Fig. 2B). Among these, five DEGs were common across multiple tissues, indicating their functional conservation. GO analysis of DEGs shared by more than three tissues revealed significant enrichment in processes such as apoptotic process, calcium ion binding, cell–cell signaling, cell adhesion, collagen-containing extracellular matrix, and extracellular region (Fig. 2C). Concurrently, KEGG pathway analysis showed that these common DEGs were significantly enriched in pathways including ECM-receptor interaction, focal adhesion, metabolic pathways, PI3K-Akt signaling pathway, TNF signaling pathway, and neuroactive ligand-receptor interaction (Fig. 2D).

#### Identification of DEPs

To identify proteins associated with prolificacy in goat, we performed a comparative proteomic analysis of ovarian tissues from animals exhibiting LF and HF lambing traits. Principal component analysis (PCA) of the proteomic profiles showed clear separation between the HF and LF groups, indicating distinct global protein expression patterns (Figure S1). Using a threshold of fold change (FC) > 1.5 or < 0.67 and a statistical significance of $p < 0.05$, we identified 286 DEPs. Among these, 143 proteins were significantly up-regulated, and 92 were significantly down-regulated in the HF group compared to the LF group (Fig. 3A and Table S8). Hierarchical clustering analysis of these DEPs revealed a clear separation

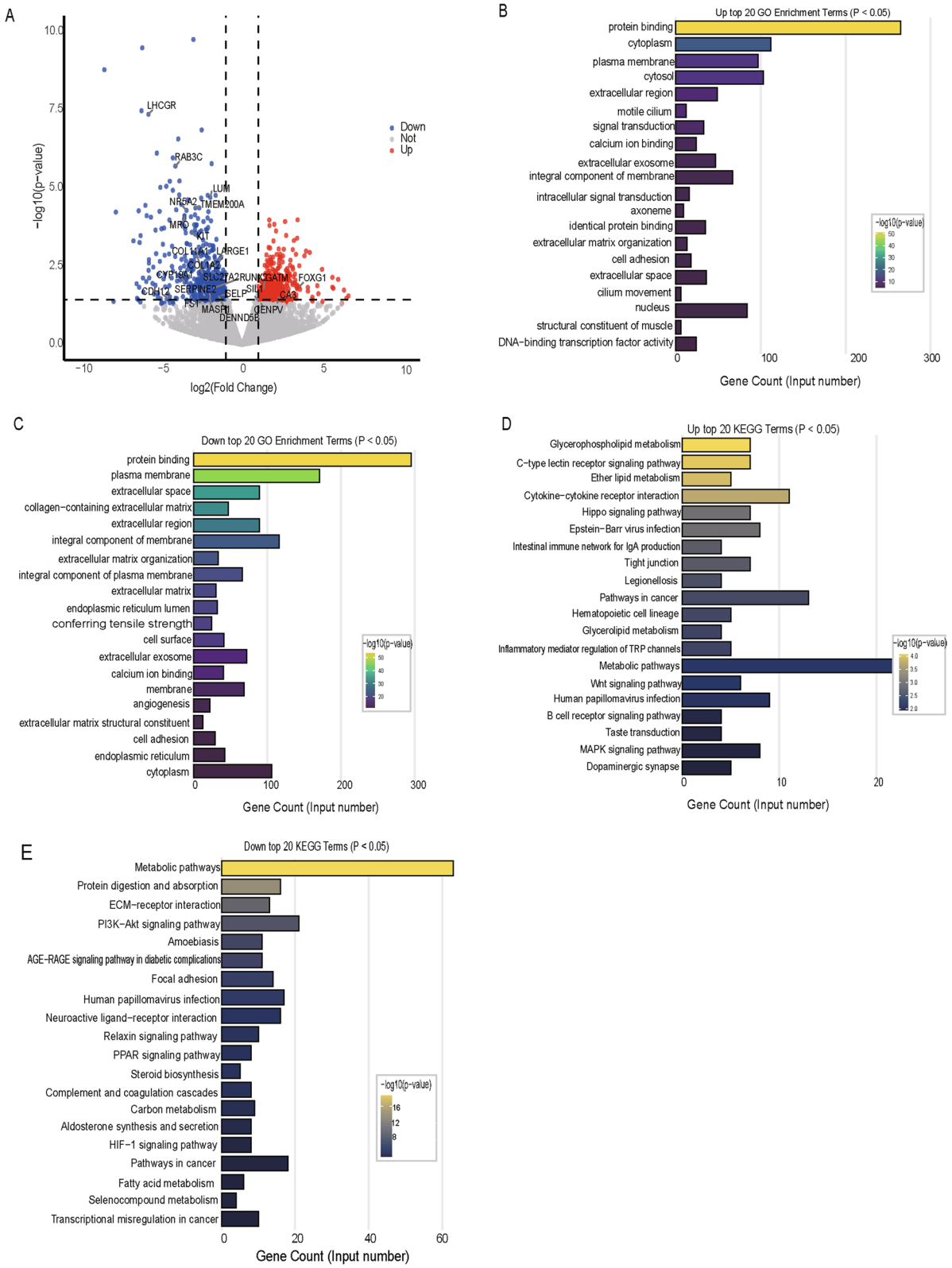


**Fig. 1** Ovarian Transcriptome Analysis of LF and HF Goats. **A** Volcano plot of differentially expressed genes (DEGs) between LF and HF goats; **B** GO enrichment analysis of up-regulated genes; **C** GO enrichment analysis of down-regulated genes; **D** KEGG enrichment analysis of up-regulated genes; **E** KEGG enrichment analysis of down-regulated genes

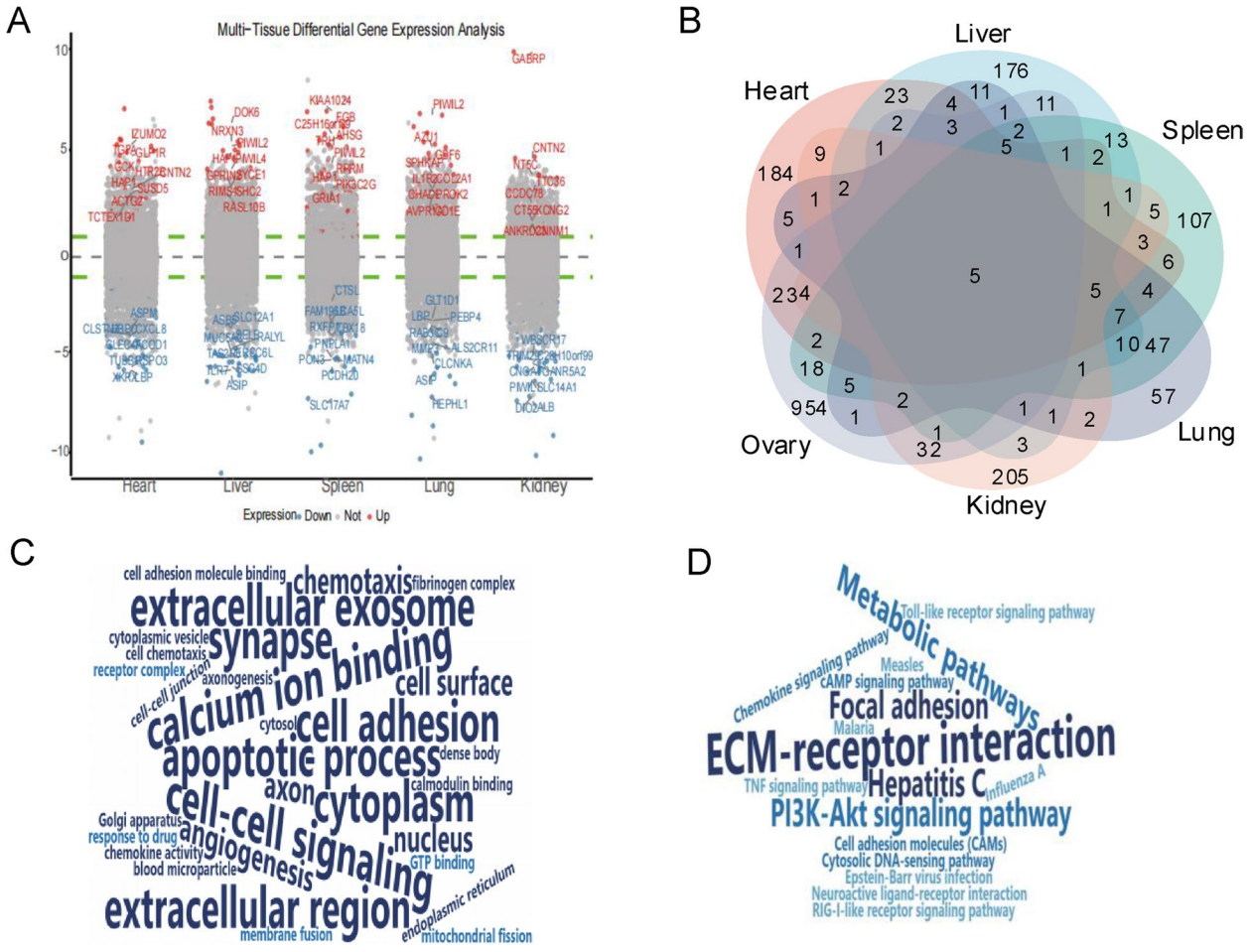


**Fig. 2** Multi-Tissue Transcriptome Atlas of LF and HF Goats. **A** Differential expression profile across multiple goat tissues; **B** Differentially expressed genes (DEGs) in multiple goat tissues; **C** GO enrichment analysis of DEGs from multiple tissues; **D** KEGG enrichment analysis of DEGs from multiple tissues

between the HF and LF groups, confirming distinct proteomic profiles associated with the two phenotypes (Fig. 3B). Subcellular localization analysis of the DEPs indicated that a majority were distributed in the nucleus (36.26%) and cytoplasm (18.13%), with significant proportions also localized to the extracellular space (12.28%) and plasma membrane (8.77%) (Figure S2). To elucidate the biological functions of these DEPs, we performed GO enrichment analysis. The up-regulated proteins were enriched in GO terms including protein binding, nucleoplasm, rRNA processing, negative regulation of apoptotic process, histone deacetylation, and cell cycle (Fig. 3C and Table S9). Conversely, the down-regulated proteins were significantly enriched in terms related to processes such as protein binding, hemoglobin biosynthetic process, localization to the plasma membrane, Golgi apparatus, negative regulation of B cell differentiation, and positive regulation of follicle-stimulating hormone secretion (Fig. 3D and Table S10). KEGG pathway analysis further revealed the key signaling and metabolic pathways involved. The up-regulated DEPs were significantly enriched in pathways such as Glycosaminoglycan biosynthesis, Base excision repair, Apoptosis, Apelin signaling pathway, Antigen processing and presentation, and Rap1 signaling pathway (Fig. 3E and Table S11). The down-regulated DEPs were enriched in pathways including Metabolic pathways, Glycosaminoglycan biosynthesis, Hippo signaling pathway, ABC transporters, N-Glycan biosynthesis, and IL-17 signaling pathway (Fig. 3F and Table S12). These results indicate that the difference in litter size is associated with extensive reprogramming of the ovarian proteome, affecting critical biological processes such as cellular structure, metabolic activity, signal transduction, and immune response. The enrichment of specific pathways like Hippo signaling and glycosaminoglycan biosynthesis suggests their potential key roles in regulating ovarian function and fecundity. A protein–protein interaction (PPI) analysis of the 286 DEPs was conducted using the STRING database. The resulting network demonstrates significant interconnectivity among the DEPs, with several hub proteins (e.g., A0A8C2S330 (*FAM169A*) and G1DFP3 (*THBS1*))

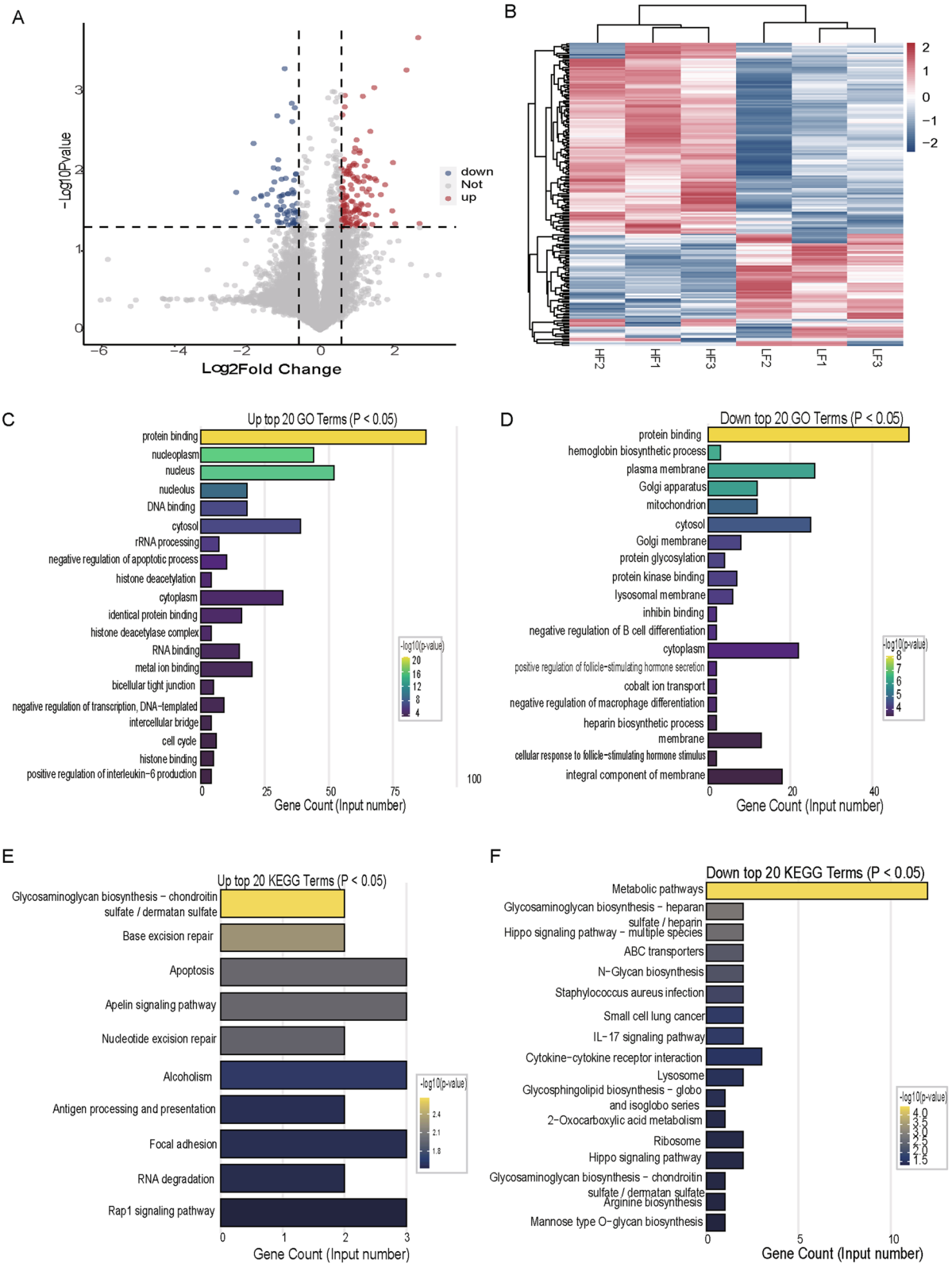


**Fig. 3** Ovarian Proteome Analysis of LF and HF Goats. **A** Volcano plot of differentially expressed proteins (DEPs) between LF and HF goats; **B** Heatmap of DEPs in LF and HF goats; **C** GO enrichment analysis of up-regulated proteins; **D** GO enrichment analysis of down-regulated proteins; **E** KEGG enrichment analysis of up-regulated proteins; **F** KEGG enrichment analysis of down-regulated proteins

exhibiting a high degree of interaction (Figure S3). Notably, the hub protein *THBS1* is annotated to participate in the TGF-β signaling pathway (Table S9), suggesting that this pathway may represent a key functional module within the ovarian proteomic network associated with prolificacy.

#### Identification of DEMs

To investigate the metabolic basis underlying prolificacy in goats, we conducted a comprehensive untargeted metabolomic analysis of serum samples with HF and LF lambing traits using both positive and negative ion modes. A total of 1,524 and 850 metabolites were identified in positive and negative ion modes, respectively. Multivariate statistical analysis using Partial Least Squares-Discriminant Analysis (PLS-DA) showed clear separation between the HF and LF in both positive (Fig. 4A and Table S13) and negative (Fig. 4B and Table S14) ion modes, indicating distinct metabolic phenotypes associated with fecundity. DEMs were screened based on the criteria of variable importance in projection (VIP) > 1.0, fold change (FC) > 1.2 or FC < 0.83, and a p-value < 0.05. In the positive ion mode, we identified 32 significantly altered metabolites, with 13 up-regulated and 19 down-regulated in the HF group compared to the LF group (Fig. 4C). In the negative ion mode, 23 metabolites were significantly altered, with 5 up-regulated and 18 down-regulated (Fig. 4D). Hierarchical clustering analysis was performed to visualize the expression patterns of significantly altered metabolites in both ionization modes. In positive ion mode, the heatmap (Fig. 4E) clearly segregated the six samples into two distinct clusters corresponding to the HF and LF groups. The 32 significantly altered metabolites (13 up-regulated and 19 down-regulated in HF) also formed two main clusters based on their expression patterns. One cluster consisted of metabolites consistently up-regulated in the HF group, including Pleuromutilin, Homochlorcyclizine, N-Acetyl-S-trans,trans-farnesyl-L-cysteine, and Cardanolide. The other cluster contained metabolites down-regulated in HF, such as Avocadene (a Fatty Acyl compound), 4-[(2,4-Dihydroxy-3,3-dimethylbutanoyl)amino]butanoic acid (a Carboxylic acid derivative), 5-Hydroxyisourate, and Epoxy(4,5Alpha)–4,5-Dihydrosantonin. This distinct clustering pattern demonstrates a strong association between these metabolic changes and the fecundity phenotype. Furthermore, correlation analysis among the significantly altered metabolites in positive ion mode revealed complex interrelationships, with both positive and negative correlations observed between different metabolite pairs (Figure S4). Similarly, in negative ion mode, the heatmap (Fig. 4F) showed clear separation between the HF and LF. The 23 significantly altered metabolites (5 up-regulated and 18 down-regulated in HF) exhibited consistent expression patterns within each group. Metabolites up-regulated in the HF group included PI(20:4(5Z,8Z,11Z,14Z)/18:0) (a Glycerophospholipid), Maresin 1, and Coagulin Q, while those down-regulated included Benzo[a]pyrene-7,8-dihydrodiol-9,10-oxide, Taurochenodeoxycholic acid, Hydroxyzine, and Moclobemide. The coherent expression patterns within each phenotypic group further validate the reliability of the identified differential metabolites. A parallel correlation analysis of metabolites detected in negative ion mode also uncovered distinct correlation patterns, highlighting potential coordinated changes within specific metabolic networks (Figure S5). KEGG pathway enrichment analysis of the differential metabolites revealed several significantly impacted metabolic pathways. In the positive ion mode, enriched pathways included Amino acid metabolism, Lipid metabolism, and Nucleotide metabolism (Fig. 4G). In the negative ion mode, significant pathways involved Amino acid metabolism, Lipid metabolism, Metabolism of cofactors and vitamins, and Xenobiotics biodegradation and metabolism (Fig. 4H). These results demonstrate that fecundity in goats is associated with significant alterations in metabolic profiles, particularly affecting lipid and amino acid metabolism pathways, which may play crucial roles in regulating reproductive performance.

#### Integrated analysis of the transcriptome, proteome and metabolome

To comprehensively elucidate the molecular mechanisms underlying fecundity in goats, we integrated transcriptomic, proteomic, and metabolomic data from ovarian tissues of goats with LH and HF lambing traits. Venn diagram analysis of DEGs and DEPs identified 3 overlapping genes/proteins (*CA3, GATM* and *CENPV*) between 533 up-regulated DEGs and 133 DEPs, and 7 overlapping genes/proteins (*SELP, RAB3C, MASP1, LARGE1, DENND5B, SLC27A2* and *TMEM200A*) between 535 down-regulated DEGs and 80 DEPs, suggesting these genes may be key targets under complex post-transcriptional regulation (Fig. 5A).The expression patterns of ten key overlapping genes were analyzed across five tissues (heart, liver, spleen, lung and kidney). This multi-tissue heatmap revealed distinct and often tissue-specific regulatory patterns for these candidate genes (Fig. 5B). For instance, the *CA3* gene was significantly up-regulated in ovarian and spleen tissues of multiple-lambing samples but down-regulated in heart tissue. The *GATM* and *CENPV* genes were nearly undetectable in other tissues and exhibited specific expression in ovarian tissue samples. Meanwhile, *SELP, RAB3C, DENND5B*, and *SLC27A2* genes showed specifically down-regulated expression in ovarian tissues of multiple-lambing samples. To further explore the cellular localization of

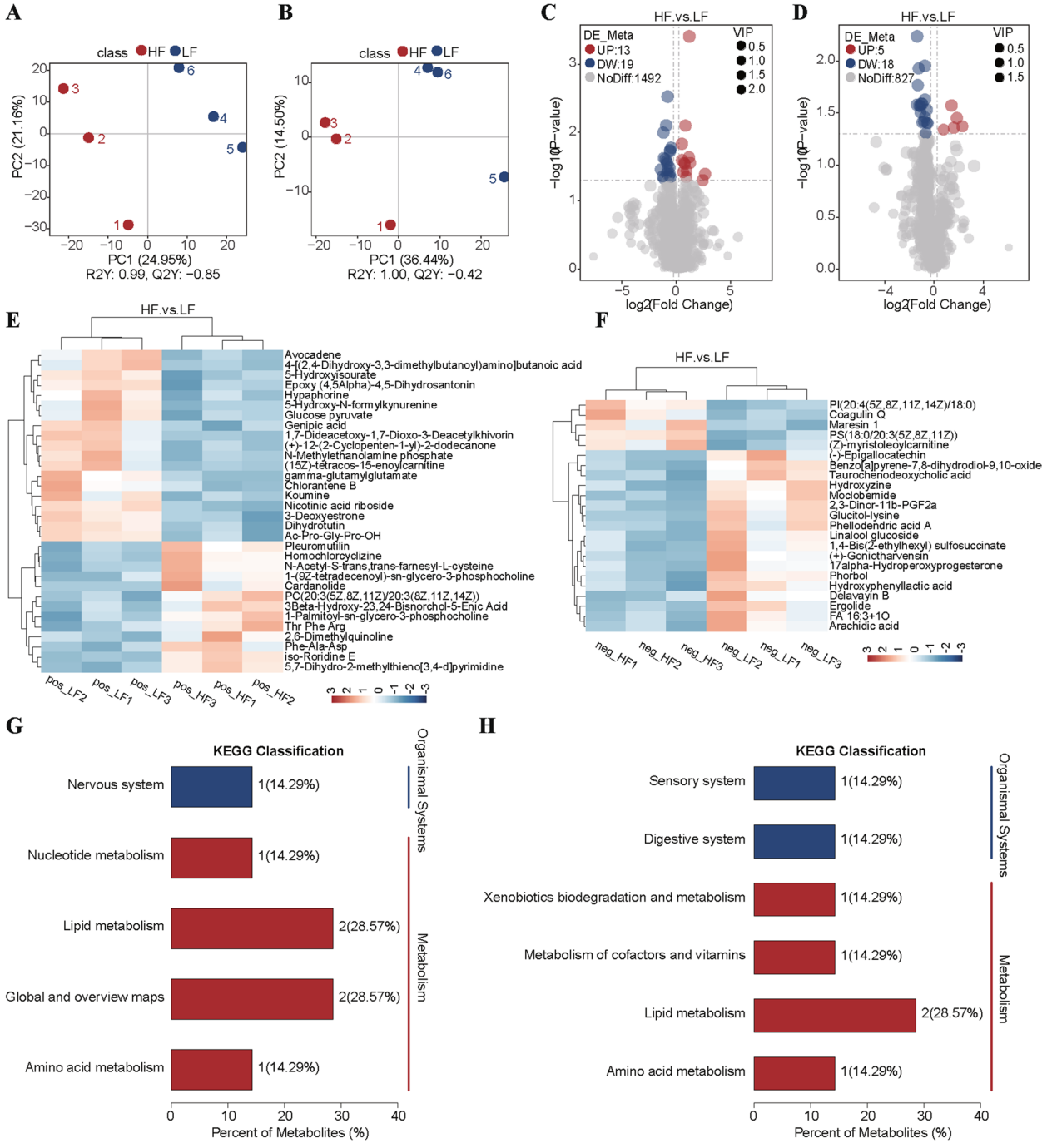


**Fig. 4** Ovarian Metabolome Analysis of LF and HF Goats. **A** PLS-DA analysis in positive ion mode; **B** PLS-DA analysis in negative ion mode; **C** Volcano plot of differential metabolites in positive ion mode; **D** Volcano plot of differential metabolites in negative ion mode; **E** Heatmap of differential metabolites in positive ion mode; **F** Heatmap of differential metabolites in negative ion mode; **G** KEGG pathway analysis of differential metabolites in positive ion mode; **H** KEGG pathway analysis of differential metabolites in negative ion mode

these key genes, we analyzed a public single-cell RNA sequencing data of goat ovarian cells [13]. The analysis revealed distinct cell-type specific expression patterns: *GATM* was specifically expressed in germ cells, while *LARGE1*, *RAB3C*, *DENND5B*, and *TMEM200A* showed specific expression in granulosa cells and internal theca cells (Fig. 5C). These expression patterns suggest important roles for these genes in follicular development. To further validate the transcriptomic data, we performed qPCR on six selected genes (3 up-regulated and 3 down-regulated) in ovarian tissue using the primer pairs listed in Table S15. The results confirmed the expression trends

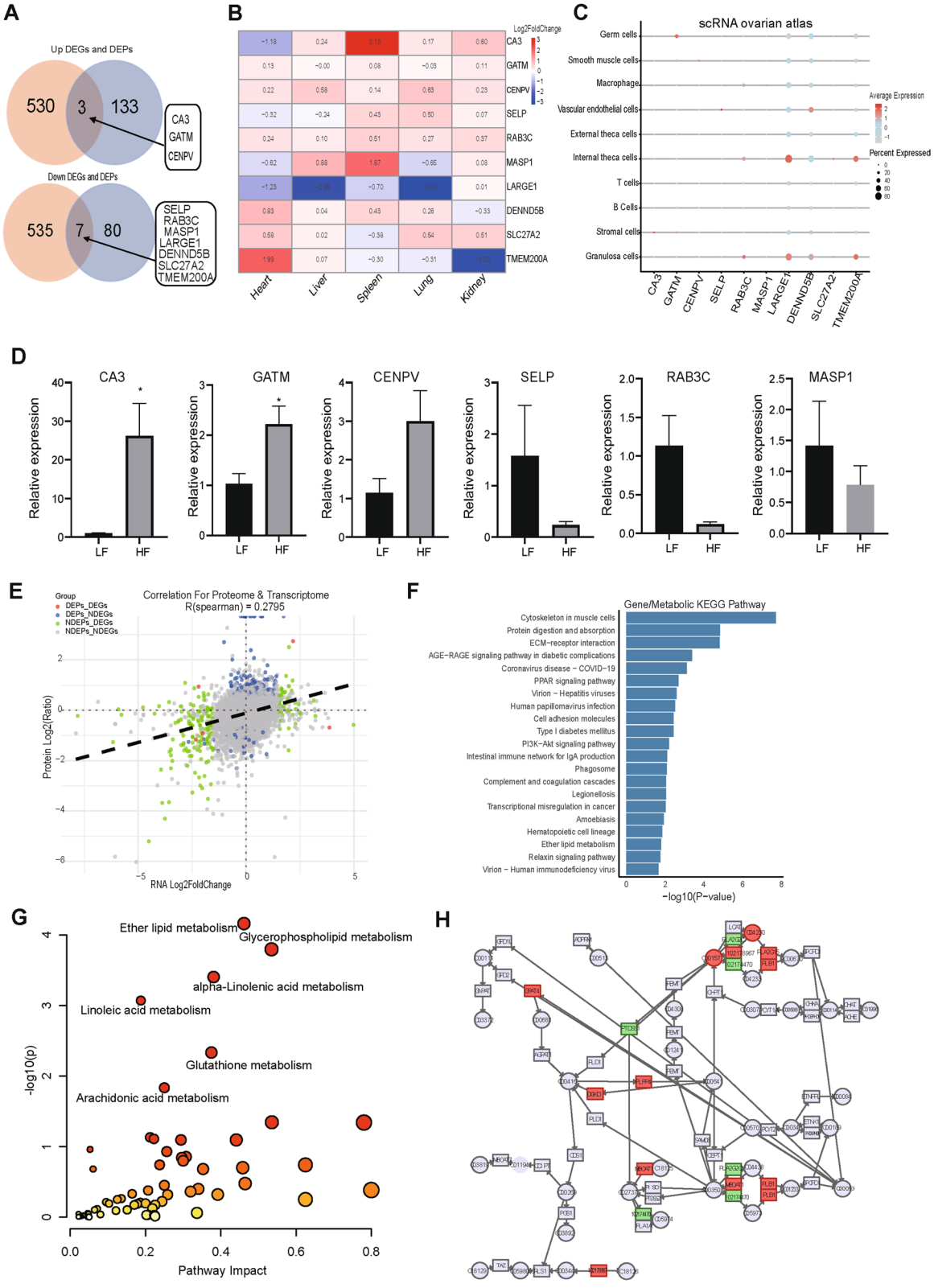


**Fig. 5** Multi-Omics Integration Analysis of LF and HF Goats. **A** Venn diagram of overlapping differentially expressed genes (DEGs) and proteins (DEPs); **B** Expression profiles of ten common DEGs/DEPs across multiple tissues; **C** Expression atlas of ten common genes in public scRNA data of goat ovaries; **D** qPCR validation of overlapping DEGs/DEPs; **E** Correlation analysis between the transcriptome and proteome; **F** Joint KEGG pathway analysis of DEGs and differential metabolites; **G** Metabolic pathway analysis of DEGs and differential metabolites; **H** Network diagram of the Glycerophospholipid metabolism pathway

observed in the RNA-seq data, thereby reinforcing the reliability of our sequencing findings (Fig. 5D).

Subsequent correlation analysis between the transcriptome and proteome in ovarian tissue revealed a weak but significant positive correlation (Spearman R = 0.2795, Fig. 5E), underscoring the moderate consistency between mRNA abundance and protein expression and hinting at prevalent post-transcriptional control mechanisms.Joint pathway enrichment analysis of the DEGs and DEMs using MetaboAnalyst highlighted several significantly enriched pathways, including the Protein digestion and absorption, ECM-receptor interaction, AGE-RAGE signaling pathway in diabetic complications, PPAR signaling pathway and PI3K-Akt signaling pathway and (Fig. 5F). Further KEGG enrichment analysis pinpointed lipid metabolism pathways as being highly impacted, with Glycerophospholipid metabolism emerging as the most significant, followed by Ether lipid metabolism, alpha-Linolenic acid metabolism, and Arachidonic acid metabolism (Fig. 5G). A detailed network map of the Glycerophospholipid metabolism pathway was constructed to visualize the interplay between key DEMs and DEGs (Fig. 5H). This analysis integrated two significantly up-regulated metabolites: PC(20:3(5Z,8Z,11Z)/20:3(8Z, 11Z,14Z)) (a Glycerophospholipid) (C00157) and 1-Palmitoyl-sn-glycero-3-phosphocholine (C04230). Concurrently, it incorporated the significantly up-regulated gene *PLA2G2C* ($\log_2$FC = 1.14) and the significantly down-regulated gene *PTDSS1* ($\log_2$FC = −1.32). The coordinated dysregulation of these specific genes and metabolites provides compelling evidence that glycerophospholipid metabolism is a central metabolic pathway intricately linked to the regulation of goat prolificacy.

## Discussion

Our multi-omics investigation provides a comprehensive and layered molecular portrait of the mechanisms underlying prolificacy in goats. The ovarian transcriptome analysis revealed 1075 DEGs between HF and LF, a substantial number that underscores the polygenic nature of this trait. It is reported that single-cell data analysis of goat and sheep ovaries revealed that genes such as *FST, CYP19A1, NR5A2, MRO, TMEM200A* and *RUNX2* have specific expressions in granulosa cells, while *COL1A2* and *LUM* are only expressed in the stromal cells and the theca cells of goat ovarian tissues, suggesting that these genes are related to follicle development [12, 13]. Notably, we identified several significantly up-regulated genes, including *CA3, CENPV*, and *VGATM*, which have not been previously reported in the context of caprine reproduction. Functional speculation on these novel genes: *CA3* activity has been detected in mammalian ovarian granulosa cells, suggesting its potential role in modulating the local pH or bicarbonate levels within the follicular fluid microenvironment, thereby influencing granulosa cell metabolism and indirectly regulating follicular development [33]. *CENPV* is crucial for proper chromosome segregation; its upregulation in high-fertility goats may indicate enhanced chromosomal stability during oocyte meiosis, supporting higher ovulation rates and embryo survival potential [34]. *VGATM* might be involved in vesicular transport of neurotransmitters or metabolites, though its specific function in the ovary remains unknown. These novel genes represent promising candidates for future functional validation studies to determine their specific roles in enhancing follicular development or ovulation rates. In addition, up-regulated genes such as *FST* and *CYP19A1*, which have been confirmed to promote the formation of dominant follicles by negatively regulating FSH secretion [13], were also identified, further supporting the relevance of the observed transcriptional changes.

The functional enrichment analysis of these DEGs was highly informative. The up-regulated genes were significantly enriched in critical signaling pathways such as the Hippo, Wnt, and MAPK pathways. The relevance of the Hippo and Wnt pathways in follicular development is supported by prior studies in other species [26–28]. Comparison with goat/sheep studies: Our findings share similarities with ovarian transcriptome studies in sheep, where pathways like Hippo, Wnt, and PI3K-Akt are also enriched in breeds with divergent fecundity. However, in contrast to many previous goat studies focused on known major reproductive genes (e.g., *BMP15, GDF9, BMPR1B*) [35], our analysis reveals a broader network of pathways and novel candidate genes, highlighting the advantage of a multi-omics approach in uncovering new regulatory layers beyond traditional candidate genes. The concurrent down-regulation of genes in the PI3K-Akt signaling pathway in our LF group suggests a potential disruption in this crucial regulatory axis, possibly leading to impaired follicular survival and maturation.

Expanding our analysis beyond the ovary to a multi-tissue transcriptomic level yielded critical insights into the systemic nature of prolificacy regulation. We discovered that the ovary harbored the highest number of tissue-specific DEGs, far exceeding those found in other tissues like the lung. This finding powerfully reinforces the ovary as the primary locus for genetic regulation of litter size. However, the identification of five DEGs that were common across multiple tissues indicates the existence of a conserved, systemic transcriptional program that coordinately supports high reproductive output [36]. These conserved genes likely participate in fundamental biological processes, such as nutrient metabolism or hormone signaling, that create a physiological state permissive for multiple ovulations. This systemic component aligns with the whole-organism energy demands of pregnancy

and lactation, suggesting that prolificacy is not merely an ovarian phenomenon but a trait supported by the integrated physiology of the animal [37].

The integration of proteomic and metabolomic data with our transcriptional findings was crucial for moving from correlation to causation and understanding functional outcomes. Joint pathway enrichment analysis identified several significantly enriched pathways, including protein digestion and absorption, ECM-receptor interaction, AGE-RAGE signaling pathway in diabetic complications, PPAR signaling pathway, and PI3K-Akt signaling pathway (Fig. 5F). These pathways are broadly implicated in cellular adhesion, energy homeostasis, and inflammatory responses, suggesting their potential roles in modulating the ovarian microenvironment critical for folliculogenesis and ovulation. Notably, the enrichment of ECM-receptor interaction and PI3K-Akt signaling pathways aligns with findings in other ruminant ovarian studies, where they are frequently associated with follicular development and steroidogenesis, underscoring their conserved importance in reproductive regulation [38, 39]. Further KEGG enrichment analysis pinpointed lipid metabolism pathways as being highly impacted, with Glycerophospholipid metabolism emerging as the most significantly altered, followed by Ether lipid metabolism, alpha-Linolenic acid metabolism, and Arachidonic acid metabolism (Fig. 5G). The central role of Glycerophospholipid metabolism was substantiated through a detailed network map (Fig. 5H), which integrated the coordinated dysregulation of two significantly up-regulated metabolites, namely PC(20:3(5Z,8Z,11Z)/20:3(8Z,11Z,14Z)) (C00157) and 1-Palmitoyl-sn-glycero-3-phosphocholine (C04230), with the significantly up-regulated gene *PLA2G2C* ($\log_2$FC = 1.14) and the significantly down-regulated gene *PTDSS1* ($\log_2$FC = –1.32). The specific dysregulation strongly implicates aberrant glycerophospholipid metabolism in potentially disrupting cellular membrane integrity, signal transduction, and energy provision within ovarian cells, thereby influencing the balance between proliferation and apoptosis. Together, these observations directly connect the systemic transcriptional clues (e.g., the cross-tissue conserved genes potentially involved in metabolism) to concrete functional metabolic disruption within the ovary. Furthermore, the PPI network of DEPs revealed that these proteins, such as the hub protein *THBS1* annotated to the TGF-β signaling pathway, are organized into interconnected modules (Figure S3). This suggests that the proteomic changes not only correlate with transcriptional and metabolic shifts but may also physically interact to execute the coordinated regulation of ovarian function. This convergence on glycerophospholipid metabolism as a core pathway regulating prolificacy is consistent with studies in other ruminants, such as sheep and cattle, where lipid metabolism pathways, including glycerophospholipid-related processes, have been linked to energy allocation, lipid storage, and reproductive performance [40]. The enrichment of the PPAR signaling pathway in our data further supports this connection, echoing its established role in lipid homeostasis and reproductive function in bovine models [41].

While our integrated multi-omics approach provides novel insights into the molecular basis of goat prolificacy, several limitations should be acknowledged. First, the sample size in this study, although consistent with previous livestock multi-omics investigations [12, 13, 18] remains relatively small, which may limit the statistical power to detect subtle molecular differences. Second, the overlap between DEGs and DEPs was limited, highlighting the complexity of post-transcriptional regulation and suggesting that future studies should incorporate additional layers of regulation (e.g., translational efficiency, protein turnover). Third, our findings are based on a single breed (Chubao black-head goats), and further validation in other prolific and non-prolific breeds is necessary to assess the generalizability of the identified pathways and candidate genes. Fourth, while we have provided detailed lambing history (Table S1), systematic data on key physiological parameters such as body condition scores were not collected. The absence of these data may limit a more comprehensive contextual interpretation of the systemic metabolic regulation suggested by our omics findings. Despite these limitations, our study establishes a foundational multi-omics resource for caprine prolificacy research. Future work should prioritize functional validation of key candidate genes using approaches such as CRISPR/Cas9-based editing in suitable models, incorporate standardized phenotyping of physiological status, and integrate additional omics layers (e.g., epigenomics, single-cell multi-omics) to further resolve the spatial and dynamic regulation of ovarian function.

## Conclusion

This study demonstrates that prolificacy in goats is governed by a multi-tiered regulatory network involving transcriptional, proteomic, and metabolic alterations. Through integrated multi-omics analysis, we identified novel candidate genes (e.g., *CA3, CENPV, GATM*) and key pathways (Hippo, Wnt, PI3K-Akt, and glycerophospholipid metabolism) that are associated with high fecundity. Multi-tissue transcriptomics revealed both ovarian-specific and systemic transcriptional adaptations. These findings advance our molecular understanding of ruminant reproduction and highlight potential targets for future research. Further experimental validation is needed before these biomarkers can be applied in breeding programs.

## Supplementary Information

The online version contains supplementary material available at https://doi.org/10.1186/s12864-026-12828-2.

Supplementary Material 1: Figure S1. PCA of the ovarian proteome profiles between HF and LF goats.

Supplementary Material 2: Figure S2. Subcellular localization of DEPs in ovarian tissues.

Supplementary Material 3: Figure S3. A protein–protein interaction analysis of the DEPs. In the interaction network, each node represents a protein, and the size of the node indicates the number of interacting proteins. The larger the node, the more proteins it interacts with. The color of the node indicates the expression level of this protein in the comparison pair. Orange represents significant high expression of this protein, and green represents significant low expression.

Supplementary Material 4: Figure S4. Correlation analysis of DEMs identified in positive ion mode.

Supplementary Material 5: Figure S5. Correlation analysis of DEMs identified in negative ion mode.

Supplementary Material 6: Table S1. Goats birth and production records. Table S2. RNA-seq analysis statistics. Table S3. Differentially expressed genes (DEGs) in LF and HF goats. Table S4. GO enrichment analysis of up-regulated genes in LF and HF goats. Table S5. GO enrichment analysis of down-regulated genes in LF and HF goats. Table S6. KEGG enrichment analysis of up-regulated genes in LF and HF goats. Table S7. KEGG enrichment analysis of down-regulated genes in LF and HF goats. Table S8. Differentially expressed proteins (DEPs) in LF and HF goats. Table S9. GO enrichment analysis of up-regulated proteins in LF and HF goats. Table S10. GO enrichment analysis of down-regulated proteins in LF and HF goats. Table S11. KEGG enrichment analysis of up-regulated proteins in LF and HF goats. Table S12. KEGG enrichment analysis of down-regulated proteins in LF and HF goats. Table S13. Differential metabolites in positive ion mode from LF and HF goats. Table S14. Differential metabolites in negative ion mode from LF and HF goats. Table S15 The qPCR primers pairs used in this study.

**Acknowledgements**
We would like to thank the reviewers for their helpful comments on the manuscript.

**Authors' contributions**
F.J. performed experiment and drafted the manuscript. H.T., M.C. and A.S. helped collect samples and analyzed data. H.L., Z.H., N.Z., F.Z., T.X., W.W., C.M. collected samples. The corresponding authors Q.X. designed this study and helped in revising the manuscript. All authors had read and approved the published version of the manuscript.

**Funding**
This project was supported by the Funds for Supporting High-Quality Development of Seed and Breeding Industry Projects in Hubei Province (HBZY2023B008), the JD Technology Research and Development Project of Hubei Province, China (2023BAA029), the Hubei Provincial Natural Science Foundation of China (2024AFB373), the Science Foundation Project of Hubei Academy of Agricultural Sciences (2024NKYJJ18 and 2026NKYJJ12), the Hubei Provincial Science and Technology Program Project (2025EBA004, 2025EBA026), and the Wuhan Science & Technology Commissioner Industry-Academia-Research Collaboration Program (2023110201030665).

**Data availability**
The raw sequence data reported in this paper have been deposited in the Genome Sequence Archive [42] in National Genomics Data Center [43], China National Center for Bioinformation/Beijing Institute of Genomics, Chinese Academy of Sciences (GSA: CRA030480) that are publicly accessible at https://ngdc.cncb.ac.cn/gsa.

## Declarations

**Ethics approval and consent to participate**
All animal experimental protocols were conformed to "The Instructive Notions with Respect to Caring for Laboratory Animals" issued by the Ministry of Science and Technology of the People's Republic of China, and approved by the Animal Care and Use Committee of Hubei Academy of Agricultural Sciences (HBAAS-2023–014).
All animal experiments were conducted with the informed consent of the owner of the lower goat farm of Hubei Academy of Agricultural Sciences.

**Consent for publication**
Not applicable.

**Competing interests**
The authors declare no competing interests.

**Author details**
[1]Key Laboratory of Animal Embryo Engineering and Molecular Breeding of Hubei Province, Institute of Animal Sciences and Veterinary Medicine, Hubei Academy of Agricultural Sciences, Wuhan 430064, China
[2]Hubei Provincial Livestock and Poultry Breeding Center, Wuhan 430064, China
[3]Wuhan Luxiang Agricultural Development Co., Ltd., Wuhan 430064, China

Received: 29 October 2025 / Accepted: 31 March 2026
Published online: 06 April 2026

**References**

1. Wang J-J, Zhang T, Chen Q-M, Zhang R-Q, Li L, Cheng S-F, et al. Genomic signatures of selection associated with litter size trait in Jining Gray goat. Front Genet. 2020;11:286.
2. Hoque M, Amin M, Baik D. Genetic and non-genetic causes of variation in gestation length, litter size and litter weight in goats. Asian-Australas J Anim Sci. 2002;15(6):772–6.
3. Kang Z, Bai Y, Lan X, Zhao H. Goat AKAP12: indel mutation detection, association analysis with litter size and alternative splicing variant expression. Front Genet. 2021;12:648256.
4. Mulsant P, Lecerf F, Fabre S, Schibler L, Monget P, Lanneluc I, et al. Mutation in bone morphogenetic protein receptor-IB is associated with increased ovulation rate in Booroola Merino ewes. Proc Natl Acad Sci USA. 2001;98(9):5104–9.
5. Ahlawat S, Sharma R, Roy M, Mandakmale S, Prakash V, Tantia M. Genotyping of novel SNPs in BMPR1B, BMP15, and GDF9 genes for association with prolificacy in seven Indian goat breeds. Anim Biotechnol. 2016;27(3):199–207.
6. Chen W, Tian Z, Lin M, Gan S, Sun W, Chu M. Expression analysis of BMPR1B, BMP15, GDF9, Smad1, Smad5, and Smad9 in rams with different fecundity. Pak J Zool. 2020;52(5):1665.
7. Wang N, Zhang G, Li M. Emerging Trends in Systems Biology: Multi-Omics Integration and Beyond. Computational Molecular Biology. 2024; 14.
8. Selby D, Jakhmola R, Sprang M, Großmann G, Raki H, Maani N, et al. Visible neural networks for multi-omics integration: a critical review. Front Artif Intell. 2025;8:1595291.
9. Shangguan A, Xiang C, Deng Z, Zhang N, Yu M, Zhang F, et al. Genome-wide association study of growth and reproductive traits based on low-coverage whole-genome sequencing in a Chubao black-head goat population. Gene. 2024;931:148891.
10. Lin Y, Sun L, Dai J, Lv Y, Liao R, Shen X, et al. Characterization and comparative analysis of whole-transcriptome sequencing in high-and low-fecundity Chongming White Goat ovaries during the estrus phase. Animals. 2024;14(7):988.
11. Pokharel K, Peippo J, Honkatukia M, Seppälä A, Rautiainen J, Ghanem N, et al. Integrated ovarian mRNA and miRNA transcriptome profiling characterizes the genetic basis of prolificacy traits in sheep (*Ovis aries*). BMC Genomics. 2018;19(1):104.
12. Ge T, Wen Y, Li B, Huang X, Jiang S, Zhang E. Single-cell sequencing reveals the reproductive variations between primiparous and multiparous Hu ewes. J Animal Sci Biotechnol. 2023;14(1):144.
13. Zhang S, Wei Y, Gao X, Song Y, Huang Y, Jiang Q. Unveiling the ovarian cell characteristics and molecular mechanism of prolificacy in goats

via single-nucleus transcriptomics data analysis. Curr Issues Mol Biol. 2024;46(3):2301–19.
14. Song Y, Zhang N, Zhang Y, Wang J, Lv Q, Zhang J. Single-cell transcriptome analysis reveals development-specific networks at distinct antral follicle stages in sheep oocytes. Int J Mol Sci. 2024;2:910.
15. Liu Z, Fu S, He X, Dai L, Liu X, Narisu, Shi C, Gu M, Wang Y, Manda. Integrated multi-tissue transcriptome profiling characterizes the genetic basis and biomarkers affecting reproduction in sheep (Ovis Aries). Genes. 2023; 14(10):1881.
16. Shl C, Liu Q, Wang W, He Q, Zhao J, Zhang F, et al. Transcriptome and proteome of ovarian revealed the differences in the ovaries of dairy goats during the breeding and non-breeding seasons. Front Vet Sci. 2025;12:1565807.
17. Shari A, Yu M, Ren X. Analysis of differential colostrum metabolism in high and low yielding Guanzhong dairy goats. Food Science of Animal Products. 2023;1:9240045.
18. Han B, Tian D, Li X, Liu S, Tian F, Liu D, et al. Multiomics analyses provide new insight into genetic variation of reproductive adaptability in tibetan sheep. Mol Biol Evol. 2024;41(3):msae058.
19. Bolger AM, Lohse M, Usadel B. Trimmomatic: a flexible trimmer for Illumina sequence data. Bioinformatics. 2014;30(15):2114–20.
20. Kim D, Langmead B, Salzberg SL. HISAT: a fast spliced aligner with low memory requirements. Nat Methods. 2015;12(4):357–60.
21. Anders S, Pyl PT, Huber W. HTSeq—a Python framework to work with high-throughput sequencing data. Bioinformatics. 2015;31(2):166–9.
22. Love MI, Huber W, Anders S. Moderated estimation of fold change and dispersion for RNA-seq data with DESeq2. Genome Biol. 2014;15(12):550.
23. Kanehisa M, Goto S. KEGG: kyoto encyclopedia of genes and genomes. Nucleic Acids Res. 2000;28(1):27–30.
24. Bu D, Luo H, Huo P, Wang Z, Zhang S, He Z, et al. KOBAS-i: intelligent prioritization and exploratory visualization of biological functions for gene enrichment analysis. Nucleic Acids Res. 2021;49(W1):W317–25.
25. Gillette MA, Satpathy S, Cao S, Dhanasekaran SM, Vasaikar SV, Krug K, et al. Proteogenomic characterization reveals therapeutic vulnerabilities in lung adenocarcinoma. Cell. 2020;182(1):200-225. e235.
26. Demichev V, Messner CB, Vernardis SI, Lilley KS, Ralser M. DIA-NN: Neural networks and interference correction enable deep coverage in high-throughput proteomics. Nat Methods. 2020:282699.
27. Franceschini A, Szklarczyk D, Frankild S, Kuhn M, Simonovic M, Roth A, et al. STRING v9.1: protein-protein interaction networks, with increased coverage and integration. Nucleic Acids Res. 2012;41(D1):D808–15.
28. Want EJ, Masson P, Michopoulos F, Wilson ID, Theodoridis G, Plumb RS, et al. Global metabolic profiling of animal and human tissues via UPLC-MS. Nat Protoc. 2013;8(1):17–32.
29. Wishart DS, Jewison T, Guo AC, Wilson M, Knox C, Liu Y, et al. HMDB 3.0—the human metabolome database in 2013. Nucleic Acids Res. 2012;41(D1):D801–7.
30. Sud M, Fahy E, Cotter D, Brown A, Dennis EA, Glass CK, et al. Lmsd: Lipid maps structure database. Nucleic Acids Res. 2007;35(suppl_1):D527–32.
31. Wen B, Mei Z, Zeng C, Liu S. metaX: a flexible and comprehensive software for processing metabolomics data. BMC Bioinformatics. 2017;18(1):183.
32. Pang Z, Lu Y, Zhou G, Hui F, Xu L, Viau C, et al. MetaboAnalyst 6.0: towards a unified platform for metabolomics data processing, analysis and interpretation. Nucleic Acids Res. 2024;52(W1):W398–406.
33. Jane Friedley N, Rosen S. Carbonic anhydrase activity in the mammalian ovary, Fallopian tube, and uterus: histochemical and biochemical studies1. Biol Reprod. 1975;12(2):293–304.
34. Nabi D, Drechsler H, Pschirer J, Korn F, Schuler N, Diez S, et al. CENP-V is required for proper chromosome segregation through interaction with spindle microtubules in mouse oocytes. Nat Commun. 2021;12(1):6547.
35. Pramod R, Sharma S, Singhi A, Pan S, Mitra A. Differential ovarian morphometry and follicular expression of BMP 15, GDF 9 and BMPR 1B influence the prolificacy in goat. Reprod Domest Anim. 2013;48(5):803–9.
36. Wang D, Tan L, Zhi Y, Bu L, Wang Y, Wang Z, et al. Genome-wide variation study and inter-tissue communication analysis unveil regulatory mechanisms of egg-laying performance in chickens. Nat Commun. 2024;15(1):7069.
37. Sun Z, Zhang Z, Liu Y, Ren C, He X, Jiang Y, et al. Integrated analysis of mRNAs and long non-coding RNAs expression of oviduct that provides novel insights into the prolificacy mechanism of goat (*Capra hircus*). Genes. 2022;13(6):1031.
38. Li D, Wu X, Chen Y, Wu Y, Abudureyimu G, Liang H, et al. Exploration of conditions for the scaled application of laparoscopic ovum pick-up in sheep and comparison of follicular development differences among breeds. Int J Mol Sci. 2025;26(5):1989.
39. Mamede G, Silveira JCD, Perrini C, Collado MD, Perecin F. The role of the PI3K-Akt signaling pathway in the developmental competence of bovine oocytes. PLoS ONE. 2017;12(9):e0185045.
40. Zhang W, Xu M, Wang J, Wang S, Wang X, Yang J, et al. Comparative transcriptome analysis of key genes and pathways activated in response to fat deposition in two sheep breeds with distinct tail phenotype. Front Genet. 2021;12:639030.
41. Liu R, Liu X, Bai X, Xiao C, Dong Y. Different expression of lipid metabolism-related genes in Shandong black cattle and Luxi cattle based on transcriptome analysis. Sci Rep. 2020;10(1):21915.
42. Chen T, Chen X, Zhang S, Zhu J, Tang B, Wang A, et al. The genome sequence archive family: toward explosive data growth and diverse data types. Genomics Proteomics Bioinformatics. 2021;19(4):578–83.
43. Database resources of the national genomics data center, China national center for bioinformation in 2025. Nucleic Acids Res. 2025;53(D1):D30-44.

## Publisher's Note